Real-time optical monitoring of radio-frequency tissue fusion by continuous wave transmission spectroscopy

Timmy Floume
Richard R. A. Syms
Imperial College
Electrical and Electronic Engineering Department
Optical and Semiconductor Device Group
Exhibition Road
London, SW7 2BT

Ara W. Darzi
George H. Hanna
St. Mary's Hospital
Biosurgery and Surgical Technology Department
South Wharf Road
London, NW2 1NY

Abstract. Radio-frequency (RF) tissue fusion is a novel method of tissue approximation that can seal tissue without the need for sutures or staples, based on the combined effects of heat and pressure on the apposed tissue surfaces. RF delivery must be controlled and optimized to obtain a reproducible, reliable seal. We use real-time optical measurements to improve understanding of the tissue modifications induced by RF fusion. The main macroscopic transformations are thermal denaturation and dehydration. Light propagation in tissue is a function of both and therefore should provide interesting insight into the dynamic of occurring phenomena. Quantification by continuous wave technique has proven challenging. We proposed an algorithm based on the measurement of the absolute transmittance of the tissue, making use of the modified Beer-Lambert law. The experimental method and the data algorithm are demonstrated by RF fusion of porcine small bowel. The proposed optical measurement modality is well adapted to modern surgical instrumentation used for minimally invasive procedures.
[DOI: 10.1117/1.3006062]

Keywords: tissue dehydration; tissue denaturation; tissue scattering; tissue absorption; RF tissue fusion; bipolar electrosurgery; modified Beer-Lambert law; transmittance spectroscopy.

Paper 08127RR received May 7, 2008; revised manuscript received Aug. 26, 2008; accepted for publication Aug. 26, 2008; published online Nov. 10, 2008.

1 Introduction

Radio frequency (RF) fusion is a new method of tissue approximation, used to seal tissue without the need for sutures or staples. This technique is now commonly used to seal blood vessel and arteries during open or laparoscopic surgery [LigaSure™ system (Valleylab, Boulder, CO, USA), BiClamp™ (ERBE, Tubingen, Germany), and Seal™ (Gyrus PK, Wokingham, UK)], and research is being carried out to transfer this vessel-sealing technology to other tissue types, such as the gastrointestinal tract.[1,2] Bowel anastamosis (for example) necessitates the approximation of bowel ends following the resection of a diseased segment, which is generally achieved by suturing or stapling. RF procedures are fast, technically undemanding, haemostatic procedures that do not introduce any foreign body (i.e., suture, staple, clip, or glue) and therefore reduce trauma and complications for the patient.

RF tissue fusion consists of clamping tissue between two electrodes while holding opposing faces under pressure. A controlled RF voltage is applied so that the induced current generates heat via the Joule effect. Tissue transformations are then induced by the combination of heat and pressure. Clearly, RF delivery and pressure must be controlled and optimized so that the transformations guarantee a reproducible, reliable seal. The main macroscopic effects induced are thermal damage and dehydration. Controlling those changes should enable the generation of a more reproducible seal and also allow optimization of the fusion process. Currently, control of RF delivery is based on the measurement of the impedance of the tissue/applicator system. In this way, the level of energy applied can be controlled via current or voltage. However, the literature on tissue impedance and especially impedance changes at a temperature similar to tissue fusion (when the boiling point of water is reached) is very sparse. Therefore, there is no consensus on how changes in impedance correlate to macroscopic transformations. There, we investigate the use of optical measurement to provide additional information on transformations. In addition, we present a spectroscopic technique and an associated data analysis procedure enabling useful information to be extracted from the optical measurement.

Numerous studies, especially in the field of light-tissue interactions, have demonstrated that thermal damage and dehydration result in the modification of tissue optical properties.[3–6] Light interacts with tissue in two ways: scattering and absorption. Scattering is due to fluctuations in the refractive index distribution at a microscopic level. Nuclei and subcellular organelles such as mitochondria, have been

Address all correspondence to: Timmy Floume, Electrical and Electronic Engineering Department, Imperial College, London, St Mary's Hospital, W2 1NY, UK. Tel: 0044 (0)790 27 64 749; Fax: 0044 (0)207 59 46 308; E-mail: t.floume@imperial.ac.uk

1083-3668/2008/13(6)/064006/8/$25.00 © 2008 SPIE

identified as the primary scattering centers.[7,8] As noted by Popp et al.,[9] the complex spatial organization of cells, organelles, fibrous domain, and extracellular matrix also contributes to scattering. Nilsson et al.[10] demonstrated an increase in the scattering coefficient of rat liver tissue after laser-induced thermotherapy, and Swartling et al.[11] noted similar changes in RF-ablated myocardium tissue. Thus, the modification of scattering properties can be used as an indicator of denaturation. Through the simultaneous measurement of absorption, chromophore content can also be assessed. Because water molecules are strongly absorbing at wavelengths of >1300 nm, the measurement of water absorption can be used to investigate hydration.

Clinical spectroscopic techniques usually involve reflectance measurement as an access to only one side of the tissue is possible. During RF fusion, the tissue faces to be sealed are sandwiched between two plane electrodes and, therefore, both sides are accessible. This enables a transmission spectroscopy arrangement to be used. The main advantage of a transmission measurement is that absolute measurement of attenuation is possible.

Here, we show that by measuring absolute transmittance during tissue fusion, we can measure absolute changes in scattering losses and water absorption, which leads respectively to the qualitative assessment of thermal damage and quantitative measurement of tissue dehydration. In Section 2, the experimental method is presented, together with the light propagation model used to extract tissue information from the transmission measurement. The results of experiments on porcine bowel are given in Section 3. In Section 4, the biophysical origins of the measured changes are discussed, and the advantages of their use as indicator of the evolving state of the tissue are described. Conclusions are presented in Section 5.

2 Material and Methods

2.1 *Experimental Arrangement*

Figure 1(a) shows a schematic of the overall measurement system. The main components are the RF delivery and optical monitoring systems.

2.1.1 *RF delivery*

The RF delivery system consisted of a generator and an applicator tool. The generator is a prototype developed by Valleylab,[2] rated at 20 V at 487 kHz. Tissue impedance is measured by continuously monitoring the voltage and current and calculating their ratio. The measured impedance is then transmitted to the data acquisition system described below. RF energy was applied to samples of thawed porcine small bowel, using two transparent electrodes ($10\times50\times1.1$ mm) made from indium tin oxide (ITO) glass (CEC020S, Praezisions Glas & Optik GmbH), as shown in Fig. 1(b). Connection to the RF generator leads was made with copper conductive tape with conductive adhesive (AT526 35 Micron Copper Foil Shielding Tape, Advance Tapes International Limited). The tissue was sandwiched between the two transparent ITO electrodes separated by two 0.5-mm-thick plastic spacers [see Fig. 1(b)]. The tissue and ITO glass were then, in turn, sandwiched between two microscope slides providing mechanical support, and bulldog clips were used to maintain the assembly.

2.1.2 *Optical monitoring*

A key objective was to investigate changes in the strong tissue water absorption band near the 1450-nm wavelength, which extends from 1350 to 1575 nm. To measure such changes in a continuous wave setup, a high-power near-infrared light source with a bandwidth sufficient to cover both the band itself and the neighboring spectral regions is required. We used a four-element superluminescent diode array (Broadlighter model Q1430, Superlum, Moscow). The emission of the overall superluminescent array is built up from overlapping spectral contributions from the four separate sources, which are combined with internal multiplexers. Figure 2 shows a typical attenuation spectrum of porcine bowel in the wavelength range covered by the superluminescent diodes.

Light from the source was coupled via a single-mode optical fiber (core diameter 8 μm) to a $20\times$ microscope objective, which formed a quasi-collimated Gaussian beam of $\approx$0.7-mm mode field diameter. This beam was passed through single layers of tissue held between the electrodes of the ITO holder Fig. 1(a). A second identical microscope objective was used to collect the transmitted light and focus it into a second single-mode optical fiber connected to an optical spectral analyzer (OSA) (Agilent AG86120). Care was taken to guarantee the collimation of the illumination beam and to ensure that the collection apparatus measured the full intensity beam in the absence of a sample, because this was a necessary condition for the absolute measurement of transmittance. The OSA was used as a detector because it can acquire spectra rapidly over a large spectral range with high sensitivity (-90 dBm) and dynamic range (120 dBm). Spectra were measured at 4.5-nm intervals between 1200 and 1650-nm wavelengths, with a resolution of 5 nm.

Spectra were exported from the OSA via a personal computer memory card international association general-purpose interface bus card (National Instrument). A software interface, developed in Labview (National Instrument), was used to display, store, and time the spectral, temperature, and impedance evolution. Complete spectra could be obtained in 600 ms.

2.1.3 *Tissue preparation*

Samples of porcine small bowel tissue (15 cm long) were obtained from a slaughterhouse washed and frozen at $-17\,^{\circ}$C. Samples frozen for no more than 4 weeks after collection were used in the experiments. Samples were thawed at room temperature and washed again to eliminate any remaining luminal content. The bowel samples were then dissected along the connection to the mesentery. A single thickness of the bowel wall was held between the jaws of the modified vessel-sealing instrument.

2.2 *Light Propagation Model*

When light propagates a distance L through a nonscattering medium (as in classic analytical spectroscopy), the Beer-Lambert law dictates the relation between the attenuation (A) and the absorption coefficient of the medium μ_a,

$$A = \mu_a L. \tag{1}$$

Here, A is the attenuation, defined as the natural logarithm of the ratio of incident to output light intensity. Measuring A and

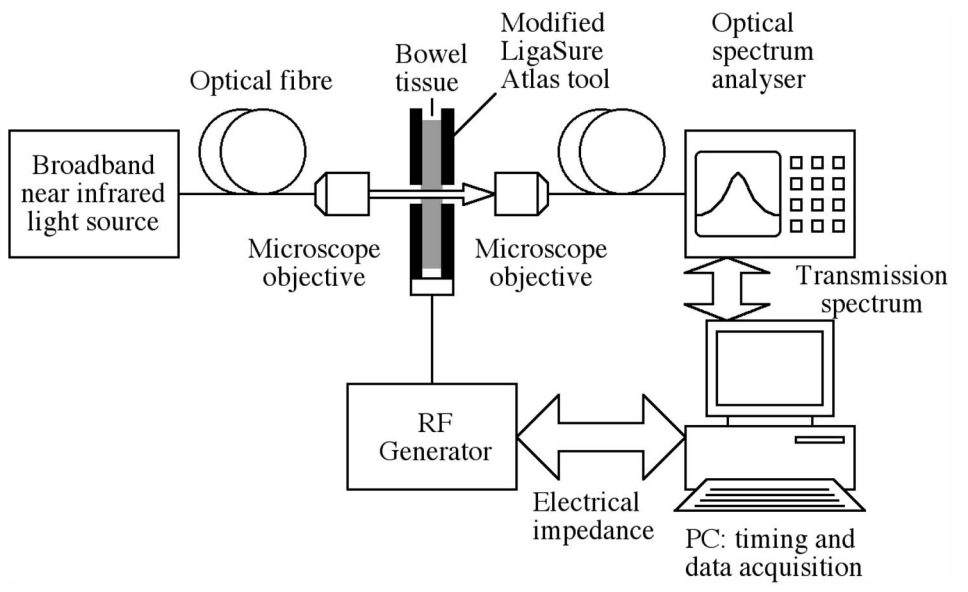

(a)

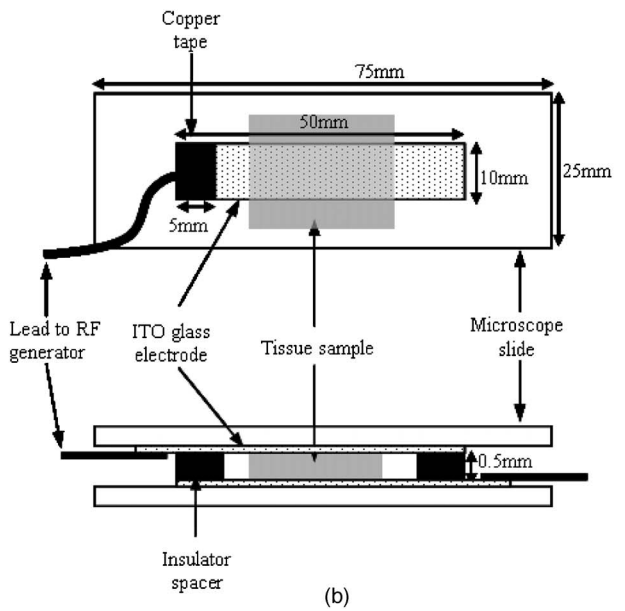

(b)

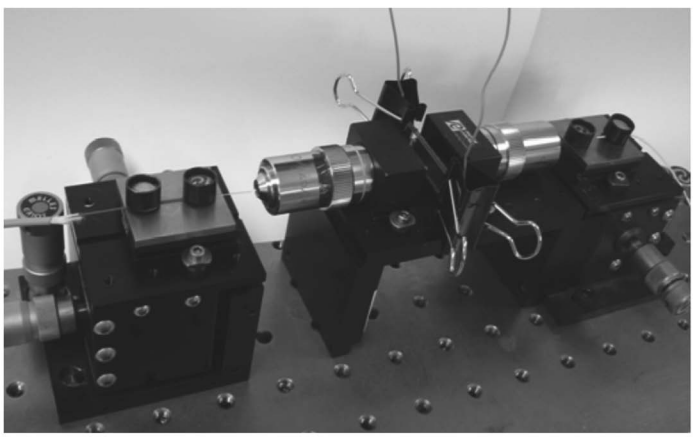

(c)

Fig. 1 (a) Schematic of continuous wave transmission spectroscopy setup, (b) schematic of the ITO glass sample holder for simultaneous light transmission and RF delivery, and (c) picture of the optical arrangement for light collection and delivery.

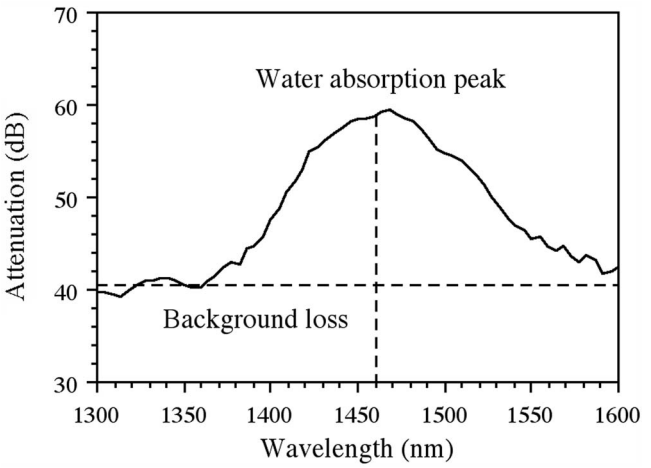

Fig. 2 Typical measured bowel water absorption band.

knowing L enables one to calculate μ_a, which is proportional to the absorber concentration. When the medium is not only absorbing but also scattering, the Beer-Lambert law must be modified to take into account the increase of optical path length.[12] Using the modified Beer-Lambert law (MBLL), the attenuation A for a scattering media can be expressed as

$$A = \mu_a BL + G \tag{2}$$

Here, B is the differential path length factor (DPF), which that expresses the average increase of the optical path of a photon in the medium and is a function of both the scattering and absorption properties. G, the scattering loss term, is a geometry-dependent factor that characterizes the reduction of light intensity due to scattering.

Without knowledge of the differential path length and scattering loss term, it is no longer possible to determine the absorption coefficient and, therefore, the absolute absorber concentration. In a typical reflectance spectroscopy geometry the scattering loss term is unknown, as it requires precise knowledge of the source/detector geometry, scattering coefficient, and exact normalisation of the attenuation by the intensity of the incident beam (so that absolute measurement of transmittance is obtained). For this reason, the MBLL has generally been used to monitor changes only in absorber concentration.[13,14]

The algorithm we present here relies on the observation that, in a transmission geometry, the absolute value of transmittance can be measured by comparing the overall transmission of a collimated beam with and without a sample. In the transmission spectrum shown in Fig. 2, it can be seen that the absorption spectrum consists of a roughly constant baseline and a strong water absorption band near 1450 nm. Applying the MBLL at wavelengths λ_1 and λ_2 inside and outside the band, we obtain

$$A(\lambda_1) = \mathrm{DPF} l \mu_a(\lambda_1) + G$$

$$A(\lambda_2) = \mathrm{DPF} l \mu_a(\lambda_2) + G. \tag{3}$$

Rearranging Eq. (3) leads to

$$G = A(\lambda_1) - \frac{\mu_a(\lambda_1)}{\mu_a(\lambda_2) - \mu_a(\lambda_1)}[A(\lambda_2) - A(\lambda_1)]. \tag{4}$$

Making the assumption that in the wavelength range of interest, tissue absorption is dominated by water absorption, we have $\mu_a(\lambda) = C_w \times \varepsilon_w(\lambda)$, where C_w is the water concentration and $\varepsilon_w(\lambda)$ the known water specific absorption at wavelength λ. Equation (4) can then be rewritten as

$$G = A(\lambda_1) - \frac{\varepsilon_w(\lambda_1)}{\varepsilon_w(\lambda_2) - \varepsilon_w(\lambda_1)}[A(\lambda_2) - A(\lambda_1)], \tag{5}$$

where all parameters are known $[\varepsilon_w(\lambda_i)]$ or measured $[A(\lambda_i)]$. Therefore, our setup enables the absolute quantification of scattering loss. Because this factor is a function of the scattering properties and geometry of the sample (i.e., its thickness) and the system (i.e., the source/detector characteristic and position). This parameter can be used qualitatively to estimate the level of thermal damage.

Assuming again that tissue absorption is dominated by water and rearranging Eq. (3), one can find the following relation between the measured attenuation and the water concentration:

$$C_w = \frac{A(\lambda_2) - A(\lambda_1)}{[\varepsilon_w(\lambda_2) - \varepsilon_w(\lambda_1)] d\mathrm{DPF}}. \tag{6}$$

We see that the absolute measurement of water concentration is possible only when the DPF is known.

We used Monte Carlo (MC) simulations in conjunction with theoretical considerations of the spatial and angular characteristics of the detected light to investigate the evolution of the DPF with a varying scattering coefficient. MC simulations were carried out using the monte carlo simulation of multilayers kedia (MCML) program, developed by Wang et al.,[12,15] which allows simulation of both the direction and position of light exiting a tissue slab made from layers with different optical property. We considered the layer of bowel tissue as optically homogeneous and simulated light propagation in a tissue slab with thickness 0.5 mm with different optical properties. The scattering coefficients simulated ranged from 50 to 500 cm^{-1}, typical of tissue scattering in its *exvivo* and thermally damaged state. The latter generally results in a two- or threefold increase of scattering coefficient.[3,6,10,17–19] The absorption coefficients (base-e) simulated correspond to 25, 50, 75, and 100% of pure water measured by Hale and Querry.[16] The anisotropy factor used for every simulation was 0.9, typical of tissue, and we assumed that this factor was constant.

To process the output of the MCML program one has to consider the influence of the measurement modality on the delivered and detected light. The angular divergence of the beam emerging from the illumination fiber was measured by a standard goniometric arrangement and the half-width of the collimated Gaussian beam created by the microscope objective derived via standard beam optic formula and found to be 0.35 mm. We therefore define the illumination beam in the MC simulation as having a Gaussian profile with the above half-width. Since the MCML program outputs the direction and position of emerging photons, we had to consider the angular and spatial conditions imposed by the optical collec-

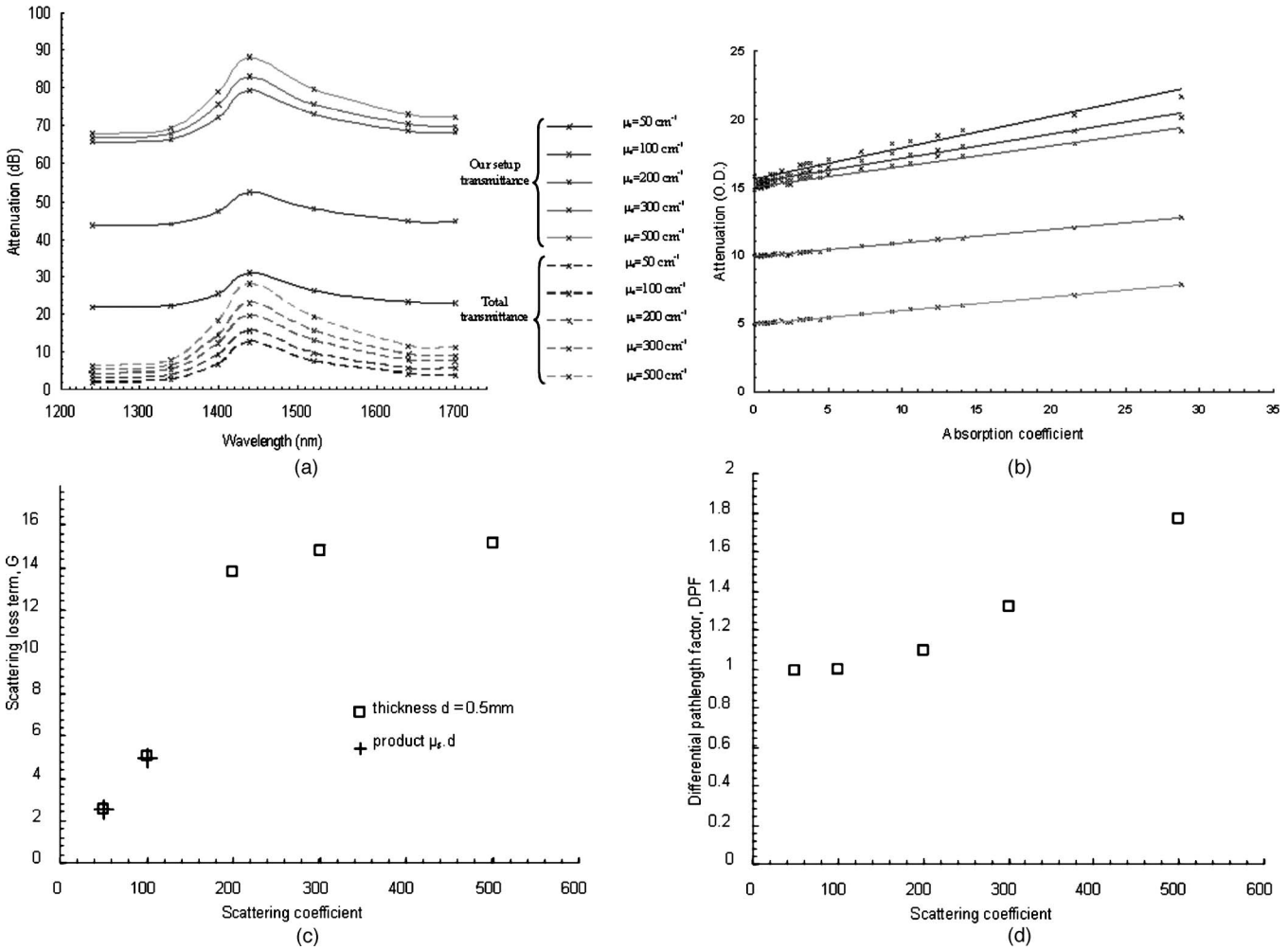

Fig. 3 (a) Results of MC simulations of attenuation spectra for different scattering coefficient and absorption coefficient of 75% of pure water, (b) simulated attenuation against absorption coefficient for different scattering coefficient, (c) scattering loss against scattering coefficient for our setup (square) and for of collimated transmission setup (cross), and (d) differential pathlength factor against scattering coefficient.

tion arrangement. When the fibre tip is positioned at the focal point of the microscope lens, the exit angle of each photon must be less than $\alpha_{max}=\tan^{-1}(R/f)$, where R is the diameter of the fiber core and f the focal length of the objective. With our experimental setup, $\alpha_{max}=5\times10^{-4}$ rad. Another condition is that output must pass through the objective, and therefore, because the exit angle is relatively small, the radial exit position must be less than the radius of the aperture stop (i.e., 2.5 mm). Accordingly, we processed the output of the MLMC program so that only photons emerging at a radius of <2.5 mm and with an angle $<5\times10^{-4}$ rad contributed to the simulated transmittance.

The results of our MC simulations are presented in Fig. 3. In Fig. 3(a), we show the evolution of the simulated total transmittance and the transmittance measured by our setup, for different values of scattering coefficient and fixed values of absorption coefficients corresponding to 75% of the absorption of pure water. The condition imposed by the collection arrangement on the measured transmittance results in a strong increase of the apparent attenuation. As scattering increases, less and less light is collected and, therefore, the attenuation baseline increases. The height of the water absorption band increases with increasing scattering. This is easily explained by the MBLL; as scattering increases, the average pathlength of light detected by the setup (i.e., the DPF) increases.

We can recast the results of the MC simulations so that the simulated attenuation is given as a function of the absorption coefficient for different values of the scattering coefficient [Fig. 3(b)], which allows the validity of the MBLL to be tested. At constant scattering coefficient, the simulated attenuation increases linearly with the absorption coefficient. This result demonstrates two important points: first, that the MBLL can be used to analyze the measurement obtained, and second, that the DPF is not a function of absorption. Therefore, the MBLL can be considered as being linear with respect to the absorption. We can therefore determine the value of the scattering loss term and DPF as the y intercept and slope of the curve of Fig. 3(b), respectively. The evolution of the scattering loss term and DPF with scattering is shown in Figs. 3(c) and 3(d), respectively.

We propose the following algorithm to extract water concentration from the measured transmittance spectra. First, one can use Eq. (5) to determine the scattering loss term (which is

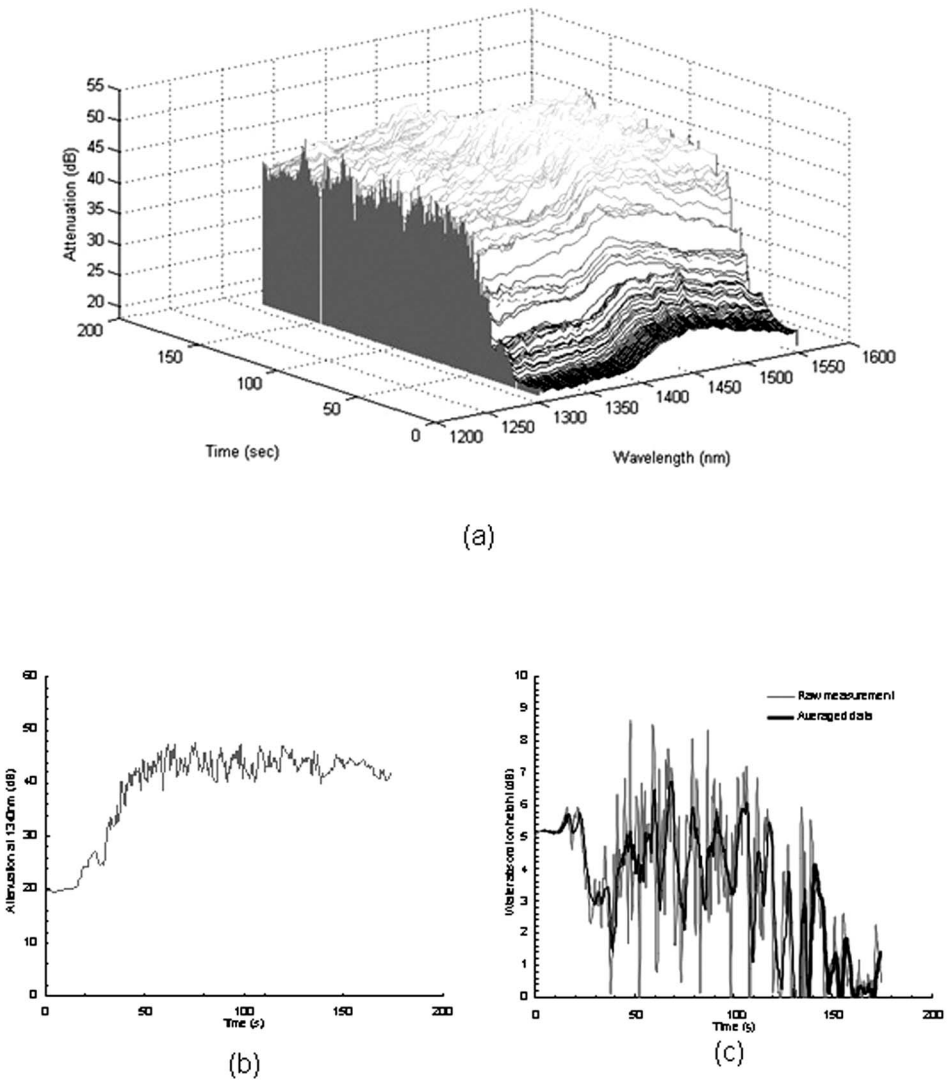

Fig. 4 Results of transmission spectroscopy during RF delivery at 20 V using ITO transparent electrodes: (a) Transmission spectra during RF delivery, (b) evolution of the attenuation baseline (measured as the attenuation at 1340 nm) against time, and (c) evolution of the water absorption band height (measured as the attenuation at 1450 nm minus the attenuation at 1340 nm) against time. Average values over the previous five spectra are also presented.

only possible when absolute transmittance is measured). One can then use this value and the results of Fig. 3(c) to determine the scattering coefficient (because the scattering loss term is a function of the setup geometry and scattering only). Now that the scattering coefficient is known, Fig. 3(d) enables one to determine the DPF, and therefore, Eq. (6) can be used to measure water concentration.

3 Results

Figure 4(a) shows the evolution of the attenuation spectra of porcine small bowel with time, during the delivery of an RF voltage of constant 20-V amplitude. Attenuation is displayed in decibels, as the base-10 logarithm of the transmittace. The time evolution of the water absorption peak and the average attenuation outside the absorption band (at 1340 nm) extracted from this data are shown in Figs. 4(b) and 4(c), respectively. Another 10 measurements showed similar evolutions.

Although under otherwise identical experimental conditions the evolution of the attenuation spectra was somewhat variable, the evolution of the attenuation baseline shows a consistent temporal characteristic, which can be divided into three phases. At the beginning of the RF application, no change in the attenuation is observed. Then the attenuation increases (until ~20 s) at all wavelengths from an initial value of 20 dB to ~40 dB. The amplitude of the water absorption peak does not change significantly, and its average value is 5 dB. After these initial phases of constant and then increasing attenuation, the height of the water absorption band becomes very variable. In Fig. 4(c), the height of the band seems to decrease rapidly just after the attenuation baseline reaches its maximum (at 20 s) and then increases for 50 s, and finally decreases again until it nearly disappears during the remaining time RF is applied. Important variation in the

water absorption height is also observed during the decreasing phase.

4 Discussion

To improve the outcome of RF tissue fusion, it is important to be able to monitor the tissue modifications involved. The experiments show that the attenuation spectra of porcine small bowel between 1300 and 1650 nm vary significantly during RF fusion. Changes were observed in both the attenuation baseline and the water absorption peak at 1450 nm, suggesting that the scattering and absorption properties of tissue are both affected.

Measurements show that the attenuation baseline increases rapidly at the start of RF delivery. The modified Beer-Lambert law suggests an increase in scattering due to the thermal damage inflicted on the tissue microstructure (a result observed in other tissue types[3,6,10,17–19]). This change only begins at the tissue coagulation temperature of $\approx 60\,^{\circ}\mathrm{C}$, which explains why very little difference is observed at the very beginning of the RF application. Therefore, changes in attenuation baseline could be suggested to assess thermal damage.

Before and at the early stage of coagulation, the water absorption is roughly constant, suggesting that tissue hydration does not quantitatively change coagulation, which is well advanced. Important variations in the absorption height are observed in the later stage of RF delivery, which suggest changes in hydration. It is still unclear if the observed variations are indeed the results of changes in hydration or an artifact of the measurement modality. Three phenomena can explain such variations. First, they may be induced by actual variations in water concentration that could be induced by fluid movements generated by water evaporation (as the tissue temperature reaches the boiling point). Second, rapid changes in the scattering properties of the tissue due to thermal damage and dehydration can induce changes in the mean optical path length of the detected light and consequently changes in the water absorption band height. Finally, these variations could be due to measurement noise, because the detected signal is close to the sensitivity limit of the OSA. Nevertheless, the results in Fig. 4 show that the disappearance of the water absorption band, and therefore tissue desiccation, can be successfully tracked during RF fusion by optical means.

In Section 2.3, we showed that, if one is able to determine the DPF during RF delivery, the absolute quantification of water content is possible via application of the MBLL. We suggested to use the absolute measurement of scattering losses, which is possible in a transmission geometry, to derive first the scattering coefficient and then the DPF. The results of MC simulations show that, as scattering increases from 50 to 200 cm^{-1}, the attenuation baseline nearly triples from $\sim$20 dB to $\sim$60 dB. As we only observed a twofold increase in attenuation baseline, we concluded that the scattering coefficient of bowel does not reach 200 cm^{-1} once thermally damaged. In this scattering range, the results shown in Fig. 3(d) suggest that the DPF stays close to unity and, therefore, that the measured water absorption band is directly proportional to tissue hydration. This result also suggests that in the scattering range considered, the geometry of the experimental setup is one of a purely collimated transmission. In Fig. 3(c), the attenuation baseline of a collimated setup (i.e., the product of the scattering coefficient by the tissue thickness) are shown as (+) for scattering coefficients of 50 and 100 cm^{-1}. Those points coincide well with the results of MC simulation, which further demonstrates that in this scattering range, we are actually measuring the collimated transmittance.

Further experimental work is necessary to assess both the applicability of the algorithm and the validity of the measurement. The former could be done by direct comparison of the results obtained by our algorithm to tissue phantoms of known scattering property and water content. The latter will necessitate the measurement of tissue state by alternative means, such as histology, to assess the degree of thermal damage and weighing of the sample to assess its level of dehydration.

5 Conclusions

We have shown that near-infrared transmission spectroscopy in the 1200–1650-nm range can allow dynamic changes in scattering loss and water absorption at 1450 nm to be characterised during RF fusion of porcine bowel tissue. During the initial stage of temperature elevation, a rise in scattering that is likely to be generated by thermal damage of tissue microstructure is observed. Once the tissue temperature reaches the boiling point of water, important variations of the water absorption height are observed. Total disappearance of the absorption band has also been observed, suggesting that tissue desiccation can be followed by transmission spectroscopy. Therefore, optical measurements show considerable potential as a modality to investigate the process of RF fusion and as feedback to control RF delivery in real time so that optimal transformations are achieved.

The analysis of our experimental data led us to devise an algorithm for absolute quantification of water content that could easily be transposed to other tissue chromophore quantification. This algorithm is mainly based on the fact that absolute attenuation measurement is possible in a transmission geometry.

Acknowledgments

The authors are extremely grateful to Tyco Healthcare for financial support and to Dr. John Carlton of Valleylab for provision of equipment and valuable technical assistance.

References

1. C. A. Shields, D. A. Schechter, P. Tetzlaff, A. L. Baily, S. Dycus, and N. Cosgriff, "Method for creating ideal tissue fusion in soft-tissue structures using radio frequency (RF) energy," *Surg. Technol. Int.* **13**, 49–55 (2004).
2. J. F. Smulders, I. H. de Hingh, J. Stavast, and J. J. Jackimowicz, "Exploring new technologies to facilitate laparoscopic surgery: Creating intestinal anastomoses without sutures or staples, using a radio-frequency-energy-driven bipolar fusion device," *Surg. Endosc* **21**, 2105–2109 (2007).
3. G. J. Derbyshire, D. K. Bogen, and M. Unger, "Thermally Induced Optical Property Changes in Myocardium at 1.06 Mu-M," *Lasers Surg. Med.* **10**(1), 28–34 (1990).
4. I. F. Cilesiz and A. J. Welch, "Light dosimetry—Effects of dehydration and thermal-damage on the optical-properties of the human aorta," *Appl. Opt.* **32**(4), 477–487 (1993).
5. J. W. Pickering, "Optical property changes as a result of protein denature in albumin and yolk," *J. Photochem. Photobiol., B* **16**(2), 101–111 (1992).
6. J. W. Pickering, S. Bosman, P. Posthumus, P. Blokland, J. F. Beek, and M. J. C. Vangemert, "Changes in the optical-properties (at

632.8 Nm) of slowly heated myocardium," *Appl. Opt.* **32**(4), 367–371 (1993).
7. J. R. Mourant, J. P. Freyer, A. H. Hielscher, A. A. Eick, D. Shen, and T. M. Johnson, "Mechanisms of light scattering from biological cells relevant to noninvasive optical-tissue diagnostics," *Appl. Opt.* **37**(16), 3586–3593 (1998).
8. B. Beauvoit, T. Kitai, and B. Chance, "Contribution of the mitochondrial compartment to the optical-properties of the rat-liver—A theoretical and practical approach," *Biophys. J.* **67**(6), 2501–2510 (1994).
9. A. K. Popp, M. T. Valentine, P. D. Kaplan, and D. A. Weitz, "Microscopic origin of light scattering in tissue," *Appl. Opt.* **42**(16), 2871–2880 (2003).
10. A. M. K. Nilsson, C. Sturesson, D. L. Liu, and S. Andersson-Engels, "Changes in spectral shape of tissue optical properties in conjunction with laser-induced thermotherapy," *Appl. Opt.* **37**(7), 1256–1267 (1998).
11. J. Swartling, S. Palsson, P. Platonov, S. B. Olsson, and S. Andersson-Engels, "Changes in tissue optical properties due to radio-frequency ablation of myocardium," *Med. Biol. Eng. Comput.* **41**(4), 403–409 (2003).
12. L. Wang, S. L. Jacques, and L. Zheng, "MCML-Monte Carlo modeling of light transport in multi-layered tissues," *Comput. Methods Programs Biomed.* **47**(2), 131–146 (1995).
13. S. J. Matcher, M. Cope, and D. T. Delpy, "Use of the water-absorption spectrum to quantify tissue chromophore concentration changes in near-infrared spectroscopy," *Phys. Med. Biol.* **39**(1), 177–196 (1994).
14. C. E. Cooper, C. E. ElWell, J. H. Meek, S. J. Matcher, J. S. Wyatt, M. Cope, and D. T. Delpy, "The noninvasive measurement of absolute cerebral deoxyhemoglobin concentration and mean optical path length in the neonatal brain by second derivative near infrared spectroscopy," *Pediatr. Res.* **39**(1), 32–38 (1996).
15. L. Wang, S. L. Jacques, and L. Zheng, "CONV—convolution for responses to a finite diameter photon beam incident on multi-layered tissues," *Comput. Methods Programs Biomed.* **54**(3), 141–50 (1997).
16. G. M. Hale and M. R. Querry, "Optical-constants of water in 200-Nm to 200-Mμm wavelength region," *Appl. Opt.* **12**(3), 555–563 (1973).
17. J. P. Ritz, A. Roggan, C. Isbert, G. Muller, H. J. Buhr, and C. T. Germer, "Optical properties of native and coagulated porcine liver tissue between 400 and 2400 nm," *Lasers Surg. Med.* **29**(3), 205–212 (2001).
18. J. P. Ritz, A. Roggan, C. Isbert, G. Muller, H. J. Buhr, and C. T. Germer, "Continuous changes in the optical properties of liver tissue during laser-induced interstitial thermotherapy" *Lasers Surg. Med.* **28**(4), 307–312 (2001).
19. G. Schuele, E. Vitkin, P. Huie, C. O'Connell-Rodwell, D. Palanker, and L. T. Perelman, "Optical spectroscopy noninvasively monitors response of organelles to cellular stress," *J. Biomed. Opt.* **10**(5), 051404–051412 (2005).